A reproducible enteric phage community improves blood glucose regulation in an obesity mouse model

Xiaotian Mao[1], Sabina Birgitte Larsen[1], Line Sidsel Fisker Zachariassen[2], Anders Brunse[3], Signe Adamberg[4], Josue Leonardo Castro Mejia[1], Kaarel Adamberg[4,5], Dennis Sandris Nielsen[1], Axel Kornerup Hansen[2], Camilla Hartmann Friis Hansen[2], Torben Sølbeck Rasmussen[1*]

Author affiliations

[1] Section of Microbiology and Fermentation, Dept. of Food Science, University of Copenhagen, Frederiksberg, Denmark

[2] Section of Experimental Animal Models, Dept. of Veterinary and Animal Sciences, University of Copenhagen, Frederiksberg, Denmark

[3] Section of Comparative Pediatrics and Nutrition, Department of Veterinary and Animal Sciences, University of Copenhagen, Frederiksberg, Denmark

[4] Department of Chemistry and Biotechnology, Tallinn University of Technology, Tallinn, Estonia

[5] Center of Food and Fermentation Technologies, Tallinn, Estonia

*Address correspondence to dn@food.ku.dk (+45 35 33 32 87) / torben@food.ku.dk (+45 35 32 80 73), Rolighedsvej 26 4th floor, 1958 Frederiksberg C, Denmark.

Keywords: Fecal virome transplantation, gut microbiome, type-2-diabetes, NAFLD, phage therapy, obesity, metabolic syndrome

Abstract

Introduction: Recent evidence suggest a link between gut microbiome dysbiosis and metabolic syndrome, including type-2-diabetes, obesity, and non-alcoholic fatty liver disease (NAFLD). Fecal microbiota transplantation (FMT) has been explored as a way to restore a healthy gut microbiome in obese patients but poses safety concerns. The wide use of FMT is limited by safety concerns about transferring the entire fecal microbiome from one individual to another. Fecal virome transplantation (FVT) is a safer alternative that transfers bacteriophages without bacterial transfer, but still carries the risk of eukaryotic virus infection. Therefore, a safer and more effective tool for modulating gut microbiome is needed.

Methods: We explored the potential of implementing three alternative FVT techniques with increased safety established in a recent study (eukaryotic viruses were either eliminated or inactivated) to ameliorate symptoms associated with a diet-induced obesity mouse model. Male mice were fed with an *ad libitum* high-fat diet before being euthanized (23 weeks of age) and received the different FVT treatments twice with one week of interval. Body weight was measured, oral glucose tests were performed, feces were sampled frequently, and liver, fat pads, mesenteric lymph node, and blood serum were sampled at termination of study.

Results: FVT treatments had no effect on weight gain or the amount of epididymal white adipose tissue. Mice given regular untreated FVT (FVT-UnT) had a significant ($p < 0.05$) drop in the pathological score of their liver tissue when compared to HFD-control mice. Mice treated with a chemostat propagated fecal virome (FVT-ChP, eukaryotic viruses eliminated by dilution) improved their blood glucose regulation significantly ($p < 0.05$) compared to HFD-control mice. Gut microbiome analysis of both the bacterial and viral component suggested that bacteriophage-mediated modulation of the gut microbiome could be a driving factor for the observed effects.

Conclusions: These results may lay the ground to develop safer bacteriophage-based therapeutic tools to restore the dysbiotic gut microbiome associated with metabolic syndrome.

Introduction

Over the past century, obesity has become a chronic metabolic disease affecting adults and children worldwide due to high-calorie foods and inadequate exercise resulting from modern lifestyles[1]. Especially, type-2-diabetes is the most common type of diabetes that are associated with obesity[2,3]. Although many obese patients can obtain substantial weight-loss, only few are able to maintain their body weight long-term[4]. It is increasingly accepted that a dysbiotic gut microbiome is highly associated to obesity[5,6] and with recurrent obesity[7]. Ridaura *et al*. revealed that fecal microbiota transplantation (FMT) from a human donor that suffered from obesity to germ-free mice resulted in a significantly increased body weight compared to germ-free mice that received FMT from a lean human donor[7,8]. While the majority of clinical experience with successful FMT comes from treating recurrent *Clostridioides difficile* infections, the application of FMT to treat obesity and type-2-diabetes remain exploratory and with limited effects[9–11]. Although the beneficial effects of FMT on intestinal pathology are well established[12], safety concerns remain associated with FMT. This was exemplified by the death of a patient in 2019 that was caused by a bacterial infection after FMT[13]. In addition to bacteria, the fecal matrix of FMT includes archaea, eukaryotes, viruses, and gut metabolome, any of which may be responsible for both the beneficial and detrimental effects of FMT[14]. Therefore, reducing the complexity of the donor fecal matrix, while maintaining its therapeutic efficacy, would be an improvement in regard to the safety in clinical settings.

The gut virome is composed of predominantly bacteriophages (in short phages) that are viruses which infect bacteria in a host-specific manner[15,16]. This ubiquitous viral entity is also prevalent in the mammalian gut microbiome and is thought to play a key role in shaping and maintaining the composition of the gut microbiome as well as affecting host metabolism[17,18]. Fecal virome transplantation (FVT, sterile filtrated donor feces) has been suggested as an alternative to FMT[16,19]. Patients suffering from recurrent *Clostridioides difficile* infections that were treated with FVT had a cure rate comparable to FMT treatment[20,21], and FVT has shown to alleviate symptoms of type-2-diabetes and obesity in mice[22], as well as preventing the onset of necrotizing enterocolitis in preterm piglets[23]. FVT has also reported to restore the gut microbiome in mice after initial disturbance with antibiotics[24]. Taken together, these findings illustrate the promising application of FVT as a treatment targeting a variety of diseases associated with gut microbiome dysbiosis. No studies have yet reported any severe adverse effects associated to FVT[21–23], however, it remains critical to ensure that no harmful microorganisms are transferred to humans when treated with FVT. The centrifugation and filtration steps applied for preparing FVT[16], cannot separate phages from eukaryotic viruses due to similar size. Screening assays can be used to detect known pathogenic viruses, but during recent years it has become evident that the human gastrointestinal tract harbors hundreds of eukaryotic viruses of unknown function[17,25,26]. Although most of these viruses are likely harmless, it should not

be neglected that they might play a key role in later disease development, as seen for the human papillomavirus (HPV) that can induce cervical cancer years after infection[27]. In two recent studies, we sought to enhance the safety of FVT by developing methodologies that selectively inactivate[28] or remove the eukaryotic viruses from the fecal matrix[29], while preserving an active gut phage community. In order to achieve this, we utilized the differences in key characteristics between eukaryotic viruses and phages[28,29]: most eukaryotic viruses are enveloped RNA viruses[30–32], and the majority of phages are non-enveloped DNA viruses[32,33]. Solvent detergent treatment was used to inactivate enveloped viruses[34], a compound (pyronin Y) that specifically binds to RNA[35,36] was applied to inactivate RNA viruses, and an optimized chemostat fermentation of fecal inoculum removed the eukaryotic viruses by dilution[29]. Some of these modified FVT viromes showed promising results in treating *Clostridioides difficile* infections in a mouse model[28], which represent a simple disease etiology that mainly is caused by the toxin producing *C. difficile*[37].

In this study we used the same modified FVTs[28] to investigate their treatment efficacy in a diet-induced obesity model[38] that represents a more complex gut microbiome associated disease, compared to *C. difficile* infections.

Results

The aim of this study was to assess potential alleviating effects of symptoms associated with type-2-diabetes and obesity by FVTs that was modified by inactivating or removing the eukaryotic viral component of the fecal viromes. We applied a solvent/detergent method (FVT-SDT) to inactivate enveloped viruses by dissolving their lipid membrane, pyronin Y treatment (FVT-PyT) to prevent RNA virus replication, and a chemostat propagated virome (FVT-ChP) to remove eukaryotic viruses by dilution. The different modified viromes were compared with an untreated virome (FVT-UnT) and saline (control) treatment of the mice fed either a high-fat (HFD-control) or low-fat diet (LFD-control). All the transferred fecal material used in the study was from the same mixed donor material.

A chemostat propagate virome improves the blood glucose clearance

The weight gain percentage of the mice was measured to evaluate the effect of the different treatments on body weight. The HFD-control mice significantly ($p < 0.05$) increased their body weight, epididymal white adipose tissue (eWAT), and insulin resistance compared to the LFD-control mice (Figure 1A, 1B, & 1C), hence, emphasizing that the diet-induced-obesity model had progressed as expected. However, the body weight and size of the eWAT was not improved by any of the FVT treatments when compared with the HFD-control group (Figure 1A and 1B). Oral glucose tolerance tests (OGTT) were performed after 13 weeks (Figure S1) and 18 weeks on high-fat diet to evaluate the insulin sensitivity of the mice. The OGTT measures of the HFD-control mice was not increased

compared to the LFD-control mice at week 13 (18 weeks of age) which indicated that the model was not yet fully effective at this stage. Neither did any of the FVT treatments show improved OGTT measured when compared with the HFD-control (Figure S1). All mice fed high-fat diet had a hampered clearance of blood glucose compared with the LFD-control mice in the first 15 min after the oral glucose administration (Figure 1D). At study week 18 (23 week of age) the blood glucose levels of mice treated with the chemostat propagated virome (FVT-ChP) decreased sharply from 30 min to 60 min after glucose administration. This highlighted a significantly ($p = 0.0429$) improved blood sugar regulation of the FVT-ChP treated mice 10 weeks after 2nd FVT treatment, compared with the HFD-control mice (Figure 1C). Although the level of blood glucose of FVT-ChP was influenced by the HFD (Figure 1C & 1D), the administration of the chemostat propagated enteric virome seemed to have contributed to an improved insulin sensitivity.

A non-alcoholic fatty liver disease (NAFLD) activity score was assessed by histopathology to evaluate the consequences of a high-fat diet on liver status (Figure 1E & Figure S2). The FVT-UnT treated mice had a significantly ($p < 0.05$) lower pathological score compared to the HFD control mice (Figure 1E). The pathological score of HFD-control, FVT-ChP, FVT-SDT, and FVT-PyT presented a significant increase ($p < 0.05$) compared with LFD-control mice.

Chemostat propagated virome treatment altered immune cell composition in fat tissue

Fluorescence-activated cell sorting (FACS) was performed to evaluate the presence of immune cells in fat tissue (Figure 2A-L) and the mesenteric lymph node (Figure S4) at termination (23 weeks of age). The mice that were treated with the chemostat propagated virome (FVT-ChP) expressed a significant ($p = 0.0331$) decrease in the number of central memory T cells CD4 (CD44+CD62I+/CD4) compared with the LFD-control (Figure 2A). The high-fat fed mice all appeared with a significant ($p < 0.05$) increase in the level of activated M1 macrophages (CD11c+/F4.80) when compared with the LFD-control group (Figure 2L). The mice treated with the untreated FVT (FVT-UnT) showed a decrease in cell number of central memory T cells CD8 ($p= 0.00314$, CD44+CD62I/CD8), dendritic cells ($p = 0.0375$, CD11c+/CD45), and M1 macrophages ($p = 0.0109$, CD11c+/F4.80) compared to the HFD-control mice (Figure 2D, 2J, & 2L). The FVT-ChP treated mice had significant ($p= 0.00371$, $p= 0.00433$) elevated levels of dendritic cells compared with FVT-UnT mice (Figure 2J).

Transplantation of modified fecal viromes shifted the gut microbiome composition

The gut bacterial and viral composition of the mice were investigated at three time points: their arrival at our housing facilities (5 weeks of age), 1 week after 2nd FVT (13 weeks of age), and at termination (23 weeks of age). Interestingly, the mice treated with the chemostat propagated virome (FVT-ChP) had significantly ($p < 0.05$) changed their gut bacterial composition compared with the HFD-control

mice and FVT-UnT treated mice at termination. Also the FVT-UnT treated mice had significantly ($p < 0.05$) changed their bacterial component at termination when compared to the HFD-control. (Figure 3B & Table S1). At termination, the relative abundance of the bacterial genus *Allobaculum* was significantly higher in FVT-ChP ($p = 0.04715$) and LFD_control ($p= 0.00144$) when compared with the HFD-control mice.

At the arrival to our housing facility the bacterial component of the mice appeared similar when analyzing the Shannon diversity index (bacterial diversity) and Bray-Curtis dissimilarity (bacterial composition) (Figure 3A and 3B). The high-fat diet had clearly ($p < 0.05$) affected the bacterial component 1 week after 2nd FVT and at termination, compared to the mice fed low-fat diet (Figure 3A & 3B). The relative abundance of *Bifidobacterium* in high-fat diet fed mice at termination was significantly lower ($p < 0.05$) than LFD-control mice, suggesting that the high-fat diet had influenced the relative abundance of *Bifidobacterium*. Meanwhile, FVT-ChP, FVT-SDT, FVT-PyT, and HFD-control mice were all composed with a significant higher ($p < 0.05$) relative abundance of *Lactobacillus* and *Lactococcus* compared with LFD-control mice.

None of the FVT treatments had affected the gut viral diversity, expressed by the Shannon diversity index, however, the viral composition (Bray-Curtis dissimilarity) of mice treated with FVT-ChP, FVT-UnT, and FVT-SDT were all significantly ($p < 0.05$) different when compared with the HFD-control mice (Figure 4A, 4B, & Table S2). More than 21.8% of the relative viral abundance could not be classified (Figure 5C). The main viral taxa represented the order *Caudovirales* (including *Podo*-, *Myo*-, and *Siphoviridae*) and the viral family of *Microviridae*. Analysis of the differential viral abundance was performed on both the level of viral contigs (vOTUs) and their predicted bacterial hosts (Figure S5 and Figure S6) to support the observed differences in the viral composition. Especially the viruses belonging to the family *Microviridae* and order *Caudovirales* were observed with significant ($p < 0.05$) differences in their relative abundance (Figure S5) while significant ($p < 0.05$) differences of the relative abundance of the predicted bacterial hosts belonged to the genera of *Parabacteroides*, *Bacteroides*, *Prevotella*, and *Akkermansia* (Figure S6) when comparing FVT-ChP and -UnT treated mice with the HFD-control at termination. This suggests that treatment with the modified viromes also affected the viral gut component of the mice over a span of 18 weeks.

Discussion

Here we addressed the safety considerations associated with the eukaryotic viral component in fecal virome transplantation (FVT) that previously have shown to alleviate symptoms of type-2-diabetes[22]. Recent developed methodologies were applied to either inactivate or remove the eukaryotic component of FVT while maintaining an active enteric phage community[28,29]. The potential effects of

alleviating symptoms of type-2-diabetes and obesity with these modified FVTs were investigated in this present study using a diet-induced obesity mouse model. The modified FVTs represented a chemostat propagated enteric virome (FVT-ChP), solvent/detergent treated fecal virome for inactivating enveloped viruses (FVT-SDT), and chemically binding of the compound pyronin Y for hindering replication of RNA viruses (FVT-PyT). Their potential alleviating effect on the diet-induced obesity model were compared with an untreated fecal virome (FVT-UnT) and a saline treatment of high-fat diet (HFD-control) and low-fat diet (LFD-control) fed control mice.

Regular FVT (equivalent to FVT-UnT) has previously been reported to reduce weight again and normalize the blood glucose regulation in a similar diet-induced obesity model[22]. However, we could not replicate these results in our study, since no clear differences in weight gain and epididymal white adipose tissue size were observed when comparing any of the FVT treatment groups with HFD control mice (Figure 1A & 1C). The FVT-UnT treated mice neither expressed improved phenotype in regard to their blood glucose regulation (Figure 1C & 1D). This is likely explained by gut microbiome differences in the donor materials that are driven by various parameters at the mouse vendor facilities which indeed challenges reproducibility[39–42]. Surprisingly, mice treated with the chemostat propagated virome (FVT-ChP) expressed a significantly ($p < 0.05$) improved blood glucose regulation compared with the HFD-Control mice. Considering the reproducibility of enteric phageome propagated with a chemostat setup (inoculated with either mouse and human inoculum)[29], this approach may constitute future perspectives to enhance the reproducibility of FVT-based studies. Most of the drug-based treatments for chronic diseases are long-term or periodic[43,44], but this study only treated mice with FVT twice. Compared with the phenotypical changes induced by a long-term high-fat diet, the two FVT treatments may be insufficient, raising the question if the number of FVT treatments should be increased in future intervention studies.

Histopathological assessment of the mouse liver tissue was performed since metabolic syndrome including obesity is highly associated with non-alcoholic fatty liver disease (NAFLD)[45]. The high-fat diet had led to NAFLD-like manifestations in the liver tissue as expected (Figure 1E, Figure S3), however, the mice treated with untreated fecal virome (FVT-UnT) had a significantly decrease in their NAFDL activity score. The fluorescence-activated cell sorting (FACS) analysis performed in this study provided valuable insights into the immune cell composition of the fat tissue of the mice in different FVT treatment groups. The FVT-UnT treated mice showed a decrease in the number of central memory T cells CD8 (CD44+CD62l/CD8), dendritic cells (CD11c+/CD45), and M1 macrophages (CD11c+/F4.80) compared with the HFD-control mice. A reduction in adipose tissue macrophages is correlated with a decrease in adipose tissue inflammation and a reduction in insulin resistance that is induced by obesity[46–48]. Additionally, dendritic cells can play a role in the immune

response to liver injury[49]. These findings suggest that FVT-UnT may have a suppressive effect on the immune response in the fat tissue of the mice which might result in a reducing liver pathology. The FACS analysis showed that mice fed a high-fat diet, except FVT-UnT mice, had a significant increase in the level of M1 macrophages (CD11c+/F4.80), which is consistent with previous studies indicating that high-fat diets promote M1 macrophage infiltration and activation in adipose tissue, leading to low-grade inflammation and insulin resistance[50].

Motived by the observed effects of the FVT-ChP and FVT-UnT treatments on, respectively, the OGTT and histology measures, the cytokine profile of the mouse blood serum was examined since low grade systemic inflammation is connected to metabolic syndrome[51,52]. The overall blood cytokine profile of the FVT-UnT treated mice was not different from the HFD-control mice, hence, these data does not explain the improved liver pathology associated with FVT-UnT compared to the HFD-control mice. In contrast, the cytokine profile of the FVT-ChP treated mice had significantly higher ($p < 0.005$) expression of several pro-inflammatory cytokines, such as IL-15, TNF-α, and MIP-2, than those of FVT-UnT, HFD-control, and LFD-control mice (Figure S7). TNF-α is produced by adipose tissue and work as pro-inflammatory cytokines that can contribute to insulin resistance and have been shown to play a role in the development of NAFLD[53–55]. In obese individuals without type-2-diabetes, a study demonstrated that inhibiting TNF-α for a duration of 6 months resulted in a reduction in fasting glucose levels[55]. The recruitment and activation of neutrophils via MIP-2 can prompt the release of diverse inflammatory mediators, which can hasten the onset of liver inflammation[56]. The increased level of several pro-inflammatory cytokines of the FVT-ChP treated mice compared to the HFD-control may be related to the pathological liver score. How and if the blood cytokine profile of the FVT-ChP treated mice was linked to the improved blood glucose regulation (Figure 1D) is unknown.

The high-fat diet decreased ($p < 0.05$) the bacterial diversity and changed the bacterial composition of the mice compared to the low-fat diet, as expected[22,57]. The FVT strongly influenced both the bacterial and viral GM composition (Table S1 & Table S2), with HFD-control mice being significantly ($p < 0.05$) different from both the FVT-UnT and FVT-ChP treated mice. The dominant bacterial phylum detected in the feces of mice were *Firmicutes*, *Bacteroidetes*, *Actinobacteria*, *Proteobacteria*, *Deferribacteres* and *Verrucomicrobia* (Figure S8). Our findings (Figure S9) revealed a significantly higher abundance of *Lactobacillus* in the gut of FVT-ChP mice compared to FVT-UnT ($p = 0.00295$), HFD-control ($p = 0.015762$), and LFD-control ($p = 0.000358$) mice. A decrease in the *Bacteroidetes*/*Firmicutes* ratio has been associated with improved metabolic health and lowered inflammation in several animal models and human studies[58–60], while increased levels of *Lactobacillus* in patients with non-alcoholic fatty liver disease (NAFLD) have been reported[61–63]. A

high relative abundance of the *Lactobacillus* taxa may partly explain the increased pro-inflammatory response and symptoms of NAFDL that was associated with the FVT-ChP treated mice (Figure 1E and Figure S7). A significant increase ($p < 0.05$) in the relative abundance of *Allobaculum* was detected in feces samples from the FVT-ChP treated mice compared to HFD-control ($p = 0.04715$) and FVT-UnT mice ($p = 0.00358$), and it was not different ($p = 0.17821$) from the relative abundance of *Allobaculum* associated with LFD-control mice (Figure S9). *Allobaculum* is a Gram-negative bacteria found in both murine and human hosts[64,65]. *Allobaculum* have been suggested to be an important gut bacterium that is inversely associated with high-fat diet induced metabolic syndrome including improved insulin response[66–68], which is in line with our observations of improved blood glucose regulation in the FVT-ChP treated mice. Differences in etiologies may explain our findings of better glucose control and reduced NAFLD in, respectively, FVT-ChP and FVT-UnT treated mice. Analysis of the differential abundance of both the viral contigs (vOTUs) and their predicted bacterial hosts showed clear differences when comparing the FVT-ChP with the FVT-UnT treatment (Figure S5 and Figure S6), hence, these differences in viral profiles may have contributes to the two different phenotypes.

Although the chemostat propagated virome (FVT-ChP) treatment promoted an inflammatory response measured in the blood serum, the FVT-ChP also showed the ability to reshape the gut microbiome composition and to improve the blood glucose regulation of the mice, likely through a cascade of events[16]. This emphasized the potential application of phage-mediated modulation of the gut microbiome to change the host phenotype.

FMT and FVT have the potential to revolutionize treatments for numerous gut-related diseases, but due to their inherent safety issues, widespread use is unlikely. Here we showed the potential of using chemostat propagated enteric viromes to improve safety of phage-mediated gut microbiome modulation that affects the host phenotype. When optimized in future studies, this approach has the potential for higher reproducibility, standardization, large-scale production, increased removal of eukaryotic viruses by further dilution, and depends on only a few effective donors.

Methods

The animal origin and preparation of donor viromes and FMT

In total 54 C57BL/6N male mice were purchased to harvest intestinal content for preparing FVT, as earlier described[28,29]. In brief, the mice were five weeks old at arrival and purchased from three vendors, represented by 18 C57BL/6NTac mice (Taconic, Denmark), 18 C57BL/6NRj mice (Janvier, France), and 18 C57BL/6NCrl mice (Charles River, Germany). Animal housing was carried out at Section of Experimental Animal Models, University of Copenhagen, Denmark, under conditions as

described previously[39]. For 13 weeks the mice were fed ad libitum low-fat diet (LF, Research Diets D12450J) until termination as 18 weeks old. To preserve the strict anaerobic bacteria for chemostat fermentation, 6 mice from each vendor (in total 18 mice) were sacrificed and immediately sampled for intestinal content under anoxic conditions. The intestinal content from the remaining mice was sampled in aerobic atmosphere to generate the fecal virome for downstream applications of the FVT-UnT, FVT-SDT, and FVT-PyT treatments. The abovementioned processes are illustrated with a flow-diagram (Figure S10). All procedures for handling of animals used for donor material were carried out in accordance with the Directive 2010/63/EU and the Danish Animal Experimentation Act with the license ID: 2012-15-2934-00256.

Untreated fecal virome (FVT-UnT)

Intestinal content from cecum and colon was thawed and processed to produce FVT solutions as previously described[22], with the exception of using Centriprep Ultracel YM-30K units (Millipore) instead of YM-50K units for concentrating filtrates and removing metabolites below the size of 30 kDa. These fecal viromes were mixed into one mixture from mice of all three vendors representing the “untreated fecal virome”, FVT-UnT, which was immediately stored at -80°C. The remaining fecal viromes were further processed to inactivate the eukaryotic viruses in the fecal viromes by either dissolving the lipid membrane of enveloped viruses with solvent/detergent (S/D) treatment or inhibit replication of RNA viruses with pyronin Y treatment.

Solvent/detergent treated fecal virome (FVT-SDT)

The solvent/detergent (S/D) treatment is commonly used for inactivating enveloped viruses (most eukaryotic viruses are enveloped) in blood plasma, while non-enveloped viruses (most phages are non-enveloped) are not inactivated[34,69,70]. The fecal viromes were treated by following the recommendations from the World Health Organization (WHO) for clinical use of S/D treated plasma; incubation in 1% (w/v) tri(n-butyl) phosphate (TnBP) and 1% (w/v) Triton X-100 at 30°C for 4 hours [71]. S/D treatment was performed by following the method of Horowitz *et al* [34] and the removal of TnBP and Triton X-100 were performed as described by Treščec *et al.*[72]. The removal of the S/D agents from the fecal viromes yielded approx. 100 mL viral-flow-through from the column which was concentrated to 0.5 mL using Centriprep Ultracel YM-30K units. The final product constituted the FVT-SDT treatment.

Pyronin Y treated fecal virome (FVT-PYT)

Pyronin Y (Merck) is a fluorescent compound (strong red-colored dye) that has been reported to efficiently bind to ss/dsRNA, while the binding to ss/dsDNA is less efficient[35,36]. Fecal filtrate was treated with 100 µM pyronin Y and incubated at 40°C overnight to inactivate viral particles containing RNA genomes. The non-bound pyronin Y molecules were removed by diluting the pyronin y treated

fecal filtrate suspensions in 50 mL SM-buffer followed by concentration to 0.5 mL with Centriprep Ultracel YM-30K units. This process was repeated three times and resulted in an almost transparent appearance of the pyronin Y-treated fecal filtrate, which constituted the FVT-PyT treatment.

Chemostat propagated fecal virome (FVT-ChP)

The preparation of the chemostat propagated virome was performed as described previously[29]. In brief, anaerobic-handled mouse cecum content was used for chemostat propagation. The culture medium was designed to mimic the LF diet (Research Diets D12450J) that the donor mice were provided as feed and the growth conditions as temperature, pH, etc. were set to mimic the environmental conditions found in mouse cecum. The end cultures fermented with a slow dilution rate (0.05 volumes 1/h) showed to generate a microbial composition closest to the donor's initial microbial composition profile[29], and these batches were mixed and constituted the applied FVT-ChP treatment.

Fluorescence microscopy

Virus-like particle (VLP) counts were evaluated of all applied fecal viromes (FVT-UnT, FVT-SDT, FVT-ChP, and FVT-PyT) by epifluorescence microscopy stained by SYBR™ Gold (Thermo Scientific, cat. no. S11494) as described dx.doi.org/10.17504/protocols.io.bx6cpraw. The viral concentration was normalized to 2 x 10^9 VLP/mL per treatment.

Animal model design

Forty-eight male C57BL/6NTac mice (Taconic Biosciences A/S, Lille Skensved, Denmark) were divided into 6 groups at 5 weeks of age: low-fat diet (LFD, as lean control), high-fat diet (HFD, as obese and prediabetic control), FVT-UnT (as control for modified FVTs), FVT-ChP, FVT-SDT, and FVT-PyT (Figure 5). Only male C57BL/6NTac mice were included since female mice are protected against DIO [73] For 18 weeks, mice were fed ad libitum a HFD (Research Diets D12492, USA), except the LFD control mice that was fed a LFD (Research Diets D12450J, USA). After 6 whole weeks on their respective diets, the FVT-UnT, FVT-ChP, FVT-SDT, and FVT-PyT mice were treated twice by FVT with 0.15 mL enteric virome by oral gavage with a 1-week interval (study weeks 7 and 8) between the FVTs. The titre of the applied FVT virome was approximately 2 × 10^9 virus-like particles (VLP)/mL (Figure S11). The mice were subjected to an oral glucose tolerance test (OGTT) at week 13 and 18 of the study, and food intake and mouse weight were monitored frequently. Procedures were carried out in accordance with the Directive 2010/63/EU and the Danish law LBK Nr 726 af 09/091993, and housing conditions as earlier described[39]. Blood serum, epididymal white adipose tissue (eWAT), mesenteric lymph node (MLN), liver tissue, intestinal content from the cecum and colon, as well as tissue from the colon and ileum were sampled at termination at study week 18 (23 weeks old) and stored at -80ºC until downstream analysis. Liver tissue was fixated in 10% neutral-

buffered formalin (Sarstedt Formalin System) for histological analysis and stored at room temperature. All procedures regarding the handling of these animals were carried out in accordance with the Directive 2010/63/EU and the Danish Animal Experimentation Act with the license ID: 2017-15-0201-01262 C1.

Cytokine analysis

Pre-weighted tissue was homogenized in 400µl lysis buffer (stock solution: 10ml Tris lysis buffer, 100µl phosphatase inhibitor 1, 100µl phosphatase inhibitor 2, and 200µl protease inhibitor (MSD inhibitor pack, Mesoscale Discovery, Rockville, MD) using a tissue blender (POLYTRON PT 1200 E, Kinematica, Luzern, Switzerland), and centrifuged (7,500g; 4°C; 5 min). Samples were diluted 1:2 and analyzed for IFN-γ, IL-1β, IL-2, IL-4, IL-5, IL-6, IL-10, IL-12p70, KC/GRO, and TNF-α with V-PLEX Proinflammatory Panel 1 Mouse kit (Mesocale Discovery) and for MIP-3α, IL-16, IL-17A, IL-17C, IL-17E, IL-17F, IL-21, IL-22, IL-23, and IL-31 with V-PLEX Th17 Panel 1 Mouse (Mesoscale Discovery) according to manufacturer's instructions. Measurements out of detection range were assigned the value of lower or upper detection limit. Concentrations were extrapolated from a standard curve and normalized to total protein measured with Pierce Detergent Compatible Bradford Assay kit according to manufacturer's protocol.

Histology

Formalin-fixed liver biopsies were embedded in paraffin, sectioned and stained with hematoxylin & eosin for histopathological evaluation. We used a cumulative semi-quantitative NAFLD activity score (NAS) comprising the following three histological features: Steatosis (0-3), immune cell margination and infiltration (0-2), and hepatocellular ballooning (0-2) with higher values corresponding to increased dissemination. The histological assessment was performed by a blinded investigator.

Cell isolation and flow cytometry (FACS)

Directly after sacrificing the mice, the mesenteric lymph node and white adipose tissue (eWAT) were placed in ice cold PBS. Single cell suspensions were prepared by disrupting the lymph node between two microscope glasses and passing it through a 70 µm nylon mesh. After washing and resuspension, 1x106 cells were surface stained for 30 min with antibodies for Percp-Cy5.5 conjugated CD11c, PE-conjugated CD86, APC-conjugated CD11b, and FITC-conjugated CD103 (all antibodies were purchased from eBiosciences) for the detection of tolerogenic dendritic cells (DCs). For the detection of T cell subsets, 1x106 cells were initially surface stained for 30 min with FITC-conjugated CD3, PercP-Cy5.5-conjugated CD4, and APC-conjugated CD8a (ebiosciences), then fixate and permeabilized with the FoxP3/Transcription Facter Staining Buffer Set (ebiosciences), and finally stained for 30 min with PE-conjugated intracellular forkhead box P3 (FOXP3) (ebioscience). Analysis was performed using an Accuri C6 flow cytometer (Accuri Cytometers).

Pre-processing of fecal samples for separation of viruses and bacteria

Fecal samples from three different timepoints were included to investigate gut microbiome changes over time: arrival at our housing facility, 1 week after 2nd FVT, and at termination. This represented in total 144 fecal samples. Separation of the viruses and bacteria from the fecal samples generated a fecal pellet and fecal supernatant by centrifugation and 0.45 µm filtering as described previously[39], however, the volume of fecal homogenate was adjusted to 5 mL SM buffer.

Bacterial DNA extraction, sequencing and pre-processing of raw data

The DNeasy PowerSoil Pro Kit (Qiagen) was used to extract bacterial DNA from the fecal pellet by following the instructions of the manufacturer. The final purified DNA was stored at -80ºC and the DNA concentration was determined using Qubit HS Assay Kit (Invitrogen, Carlsbad, California, USA) on the Qubit 4 Fluorometric Quantification device (Invitrogen, Carlsbad, California, USA). The bacterial community composition was determined by Illumina NextSeq-based high-throughput sequencing (HTS) of the 16S rRNA gene V3-region, as previously described [39]. Quality-control of reads, de-replicating, purging from chimeric reads and constructing zOTU was conducted with the UNOISE pipeline [74] and taxonomically assigned with Sintax [75] (not yet peer reviewed). Taxonomical assignments were obtained using the EZtaxon for 16S rRNA gene database[76]. Code describing this pipeline can be accessed in github.com/jcame/Fastq_2_zOTUtable. The average sequencing depth after quality control (Accession: PRJEB58786, available at ENA) for the fecal 16S rRNA gene amplicons was 67,454 reads (min. 12,790 reads and max. 295,746 reads).

Viral RNA/DNA extraction, sequencing and pre-processing of raw data

The sterile filtered fecal supernatant was concentrated using centrifugal filters Centrisart with a filter cut-off at 100 kDA (Sartorius) by centrifugation centrifuged at 1,500 x g at 4ºC

(dx.doi.org/10.17504/protocols.io.b2qaqdse). The viral DNA/RNA was extracted from the fecal supernatants with Viral RNA mini kit (Qiagen) as previously described[39]. Reverse transcription was executed with SuperScript VILO Master mix by following the instructions of the manufacturer and subsequently cleaned with DNeasy blood and tissue kit (Qiagen) by only following step 3-8. In brief, the DNA/cDNA samples were mixed with ethanol, bound to the silica filter, washed two times, and eluted with 40 µL elution buffer. Multiple displacement amplification (MDA, to include ssDNA viruses) using GenomiPhi V3 DNA amplification kit (Cytiva) and sequencing library preparation using Nextera XT kit was performed at previously described[39], and send for sequencing using the NovaSeq platform (NovoGene). The average sequencing depth of raw reads (Accession: PRJEB58786, available at ENA) for the fecal viral metagenome was 13,145,283 reads (min. 693,882 reads and max. 142,821,858 reads. The raw reads were trimmed from adaptors and the high-quality sequences (>95% quality) using Trimmomatic v0.35[77] with a minimum size of 50nt were retained for further analysis. High quality reads were de-replicated and checked for the presence of PhiX control using BBMap (bbduk.sh) (https://www.osti.gov/servlets/purl/1241166). Virus-like particle-derived DNA sequences were subjected to within-sample de-novo assembly-only using Spades v3.13.1[78] and the contigs with a minimum length of 2,200 nt, were retained. Contigs generated from all samples were pooled and de-replicated at 90% identity using BBMap (dedupe.sh). Prediction of viral contigs/genomes was carried out using VirSorter2[79] ("full" categories | dsDNAphage, ssDNA, RNA, Lavidaviridae, NCLDV | viralquality ≥ 0.66), vibrant[80] (High-quality | Complete), and checkv[81] (High-quality | Complete). Taxonomy was inferred by blasting viral ORF against viral orthologous groups (https://vogdb.org) and the Lowest Common Ancestor (LCA) for every contig was estimated based on a minimum e-value of $10e^{-5}$. Phage-host prediction was determined by blasting (85% identity) CRISPR spacers and tRNAs predicted from >150,000 gut species-level genome bins (SGBs)[82,83] ([83], not yet peer reviewed). Following assembly, quality control, and annotations, reads from all samples were mapped against the viral (high-quality) contigs (vOTUs) using the bowtie2[84] and a contingency-table of reads per Kbp of contig sequence per million reads sample (RPKM) was generated, here defined as vOTU-table (viral contigs). Code describing this pipeline can be accessed in github.com/jcame/virome_analysis-FOOD.

Bioinformatic analysis of bacterial and viral sequences

Initially the dataset was purged for zOTU's/viral contigs, which were detected in less than 5% of the samples, but the resulting dataset still maintained 99.5% of the total reads. Cumulative sum scaling (CSS)[85] was applied for the analysis of beta-diversity to counteract that a few zOTU/viral contigs represented a majority of count values, since CSS have been benchmarked with a high accuracy for the applied metrics[86]. CSS normalization was performed using the R software using the

metagenomeSeq package[87]. R version 4.2.2[88] was used for subsequent analysis and presentation of data. The main packages used were phyloseq[89], vegan[90], deseseq2[91], ampvis2[92], ggpubr[93] and ggplot2[93]. A-diversity analysis was based on raw read counts and statistics were based on ANOVA. B-diversity was represented by Bray Curtis dissimilarity and statistics were based on PERMANOVA. T-test with pooled standard deviations was applied to assess the statistically differences between the treatment groups of cytokine levels, immune cell levels, eWAT, bodyweight, and histology. Mouse data (weight and OGTT levels) were analyzed in GraphPad Prism using one-way analysis of variance with Tukey's post hoc test.

Acknowledgements

We thank the animal caretakers Helene Farlov and Mette Nelander at Section of Experimental Animal Models (University of Copenhagen, Denmark) for taking care of the animals during the study and assisting with the animal handling.

Funding

Funding was provided by the Lundbeck Foundation with grant ID: R324-2019-1880 under the acronym "SafeVir" and the Novo Nordisk Foundation with grant ID: NNF-20OC0063874 under the acronum "PrePhage".

Author contributions

TSR and DSN conceived the research idea and designed the study; TSR and SBL, performed the experiments; TSR, SBL, XM, LSFZ, AB, SA, JLCM, CHFH, KA, and AKH performed laboratory and data analysis; XM and TSR wrote the first draft of the manuscript. All authors critically revised and approved the final version of the manuscript.

Competing interests

All authors declare no conflicts of interest.

References

1. Kyrou, I.; Randeva, H.S.; Tsigos, C.; Kaltsas, G.; Weickert, M.O. Clinical Problems Caused by Obesity. In Endotext; Feingold, K.R., Anawalt, B., Boyce, A., Chrousos, G., de Herder, W.W., Dhatariya, K., Dungan, K., Hershman, J.M., Hofland, J., Kalra, S., e et al. World Health Organization. World Obesity Day 2022—Accelerating Action to Stop Obesity. 2022;

2. Leitner DR, Frühbeck G, Yumuk V, Schindler K, Micic D, Woodward E, Toplak H. Obesity and Type 2 Diabetes: Two Diseases with a Need for Combined Treatment Strategies - EASO Can Lead the Way. Obes Facts 2017; 10:483–92.

3. Yumuk V, Tsigos C, Fried M, Schindler K, Busetto L, Micic D, Toplak H, Obesity Management Task Force of the European Association for the Study of Obesity. European Guidelines for Obesity Management in Adults. Obes Facts 2015; 8:402–24.

4. Blomain ES, Dirhan DA, Valentino MA, Kim GW, Waldman SA. Mechanisms of Weight Regain following Weight Loss. ISRN Obes 2013; 2013:1–7.

5. Maruvada P, Leone V, Kaplan LM, Chang EB. The Human Microbiome and Obesity: Moving beyond Associations. Cell Host Microbe 2017; 22:589–99.

6. Bäckhed F, Manchester JK, Semenkovich CF, Gordon JI. Mechanisms underlying the resistance to diet-induced obesity in germ-free mice. Proc Natl Acad Sci U S A 2007; 104:979–84.

7. Thaiss CA, Itav S, Rothschild D, Meijer MT, Levy M, Moresi C, Dohnalová L, Braverman S, Rozin S, Malitsky S, et al. Persistent microbiome alterations modulate the rate of post-dieting weight regain. Nature [Internet] 2016; 540:544–51. Available from: http://www.nature.com/articles/nature20796

8. Ridaura VK, Faith JJ, Rey FE, Cheng J, Duncan AE, Kau AL, Griffin NW, Lombard V, Henrissat B, Bain JR, et al. Gut microbiota from twins discordant for obesity modulate metabolism in mice. Science 2013; 341:1241214.

9. Lahtinen P, Juuti A, Luostarinen M, Niskanen L, Liukkonen T, Tillonen J, Kössi J, Ilvesmäki V, Viljakka M, Satokari R, et al. Effectiveness of Fecal Microbiota Transplantation for Weight Loss in Patients With Obesity Undergoing Bariatric Surgery. JAMA Netw Open 2022; 5:e2247226.

10. Allegretti JR, Kassam Z, Mullish BH, Chiang A, Carrellas M, Hurtado J, Marchesi JR, McDonald JAK, Pechlivanis A, Barker GF, et al. Effects of Fecal Microbiota Transplantation With Oral Capsules in Obese Patients. Clin Gastroenterol Hepatol 2020; 18:855-863.e2.

11. Yu EW, Gao L, Stastka P, Cheney MC, Mahabamunuge J, Soto MT, Ford CB, Bryant JA, Henn MR, Hohmann EL. Fecal microbiota transplantation for the improvement of metabolism in obesity: The FMT-TRIM double-blind placebo-controlled pilot trial. PLoS Med 2020; 17.

12. Wang J-W, Kuo C-H, Kuo F-C, Wang Y-K, Hsu W-H, Yu F-J, Hu H-M, Hsu P-I, Wang J-Y, Wu D-C. Fecal microbiota transplantation: Review and update. Journal of the Formosan Medical Association 2019; 118:S23–31.

13. FDA. Important safety alert regarding use of FMT [Internet]. 2019 [cited 2019 Jul 4]; Available from: https://www.fda.gov/vaccines-blood-biologics/safety-availability-

biologics/important-safety-alert-regarding-use-fecal-microbiota-transplantation-and-risk-serious-adverse

14. Marotz CA, Zarrinpar A. Treating Obesity and Metabolic Syndrome with Fecal Microbiota Transplantation. Yale J Biol Med 2016; 89:383–8.

15. Ross A, Ward S, Hyman P. More Is Better: Selecting for Broad Host Range Bacteriophages. Front Microbiol 2016; 7:1–6.

16. Rasmussen TS, Koefoed AK, Jakobsen RR, Deng L, Castro-Mejía JL, Brunse A, Neve H, Vogensen FK, Nielsen DS. Bacteriophage-mediated manipulation of the gut microbiome - promises and presents limitations. FEMS Microbiol Rev 2020; 44:507–21.

17. Lim ES, Zhou Y, Zhao G, Bauer IK, Droit L, Ndao IM, Warner BB, Tarr PI, Wang D, Holtz LR. Early life dynamics of the human gut virome and bacterial microbiome in infants. Nat Med 2015; 21:1228–34.

18. Liang G, Zhao C, Zhang H, Mattei L, Sherrill-Mix S, Bittinger K, Kessler LR, Wu GD, Baldassano RN, DeRusso P, et al. The stepwise assembly of the neonatal virome is modulated by breastfeeding. Nature 2020; 581:470–4.

19. Wu D, Zhang C, Liu Y, Yao J, Yang X, Wu S, Du J, Yang X, Wu D, Zhang C, et al. Beyond faecal microbiota transplantation, the non-negligible role of faecal virome or bacteriophage transplantation. Journal of Microbiology, Immunology and Infection [Internet] 2023 [cited 2023 Mar 10]; Available from: http://creativecommons.org/licenses/by-nc-nd/4.0/

20. Kao DH, Roach B, Walter J, Lobenberg R, Wong K. Effect of lyophilized sterile fecal filtrate vs lyophilized donor stool on recurrent Clostridium difficile infection (rCDI): Prelimenary results from a randomized, double-blind pilot study. J Can Assoc Gastroenterol 2019; 2:101–2.

21. Ott SJ, Waetzig GH, Rehman A, Moltzau-Anderson J, Bharti R, Grasis JA, Cassidy L, Tholey A, Fickenscher H, Seegert D, et al. Efficacy of Sterile Fecal Filtrate Transfer for Treating Patients With Clostridium difficile Infection. Gastroenterology 2017; 152:799-811.e7.

22. Rasmussen TS, Mentzel CMJ, Kot W, Castro-Mejía JL, Zuffa S, Swann JR, Hansen LH, Vogensen FK, Hansen AK, Nielsen DS. Faecal virome transplantation decreases symptoms of type 2 diabetes and obesity in a murine model. Gut [Internet] 2020 [cited 2020 Mar 13]; 69:2122–30. Available from: https://doi.org/10.1136/gutjnl-2019-320005

23. Brunse A, Deng L, Pan X, Hui Y, Castro-Mejía JL, Kot W, Nguyen DN, Secher JB-M, Nielsen DS, Thymann T. Fecal filtrate transplantation protects against necrotizing enterocolitis. ISME J 2022; 16:686–94.

24. Draper LA, Ryan FJ, Dalmasso M, Casey PG, McCann A, Velayudhan V, Ross RP, Hill C. Autochthonous faecal viral transfer (FVT) impacts the murine microbiome after antibiotic perturbation. BMC Biol 2020; 18:173.

25. Cao Z, Sugimura N, Burgermeister E, Ebert MP, Zuo T, Lan P. The gut virome: A new microbiome component in health and disease. EBioMedicine 2022; 81:104113.

26. Shah SA, Deng L, Thorsen J, Pedersen AG, Dion MB, Castro-Mejía JL, Silins R, Romme FO, Sausset R, Ndela EO, et al. Hundreds of viral families in the healthy infant gut. bioRxiv 2022;

27. Doorbar J, Egawa N, Griffin H, Kranjec C, Murakami I. Human papillomavirus molecular biology and disease association. Rev Med Virol 2015; 25:2–23.

28. Rasmussen TS, Forster S, Larsen SB, Von Münchow A, Tranæs KD, Brunse A, Castro-Mejia JL, Adamberg S, Hansen AK, Adamberg K, et al. Development of safe and effective bacteriophage-mediated therapies against C. difficile infections – a proof-of-concept preclinical study . bioRxiv 2023;

29. Adamberg S, Rasmussen TS, Larsen SB, Nielsen DS, Adamberg K. Reproducible chemostat cultures to eliminate eukaryotic viruses from fecal transplant material. bioRxiv 2023;

30. Rey FA, Lok S-M. Common Features of Enveloped Viruses and Implications for Immunogen Design for Next-Generation Vaccines. Cell 2018; 172:1319–34.

31. Bell PJL. Evidence supporting a viral origin of the eukaryotic nucleus. Virus Res 2020; 289:198168.

32. Koonin E V., Dolja V V., Krupovic M. Origins and evolution of viruses of eukaryotes: The ultimate modularity. Virology2015; 479–480:2–25.

33. Sausset R, Petit MA, Gaboriau-Routhiau V, De Paepe M. New insights into intestinal phages. Mucosal Immunol 2020; 13:205–15.

34. Horowitz B, Bonomo R, Prince AM, Chin SN, Brotman B, Shulman RW. Solvent/detergent-treated plasma: a virus-inactivated substitute for fresh frozen plasma. Blood 1992; 79:826–31.

35. Kapuscinski J, Darzynkiewicz Z. Interactions of pyronin Y(G) with nucleic acids. Cytometry 1987; 8:129–37.

36. Darzynkiewicz Z, Kapuscinski J, Carter SP, Schmid FA, Melamed MR. Cytostatic and cytotoxic properties of pyronin Y: relation to mitochondrial localization of the dye and its interaction with RNA. Cancer Res 1986; 46:5760–6.

37. Rao K, Erb-Downward JR, Walk ST, Micic D, Falkowski N, Santhosh K, Mogle JA, Ring C, Young VB, Huffnagle GB, et al. The Systemic Inflammatory Response to Clostridium difficile Infection. PLoS One 2014; 9:e92578.

38. Fraulob JC, Ogg-Diamantino R, Fernandes-Santos C, Aguila MB, Mandarim-de-Lacerda CA. A Mouse Model of Metabolic Syndrome: Insulin Resistance, Fatty Liver and Non-Alcoholic Fatty Pancreas Disease (NAFPD) in C57BL/6 Mice Fed a High Fat Diet. J Clin Biochem Nutr 2010; 46:212–23.

39. Rasmussen TS, de Vries L, Kot W, Hansen LH, Castro-Mejía JL, Vogensen FK, Hansen AK, Nielsen DS. Mouse Vendor Influence on the Bacterial and Viral Gut Composition Exceeds the Effect of Diet. Viruses 2019; 11.

40. Ericsson AC, Davis JW, Spollen W, Bivens N, Givan S, Hagan CE, McIntosh M, Franklin CL. Effects of vendor and genetic background on the composition of the fecal microbiota of inbred mice. PLoS One 2015; 10:1–19.

41. Lundberg R, Bahl MI, Licht TR, Toft MF, Hansen AK. Microbiota composition of simultaneously colonized mice housed under either a gnotobiotic isolator or individually ventilated cage regime. Sci Rep 2017; 7:1–11.

42. Rasmussen TS, Jakobsen RR, Castro-Mejía JL, Kot W, Thomsen AR, Vogensen FK, Nielsen DS, Hansen AK. Inter-vendor variance of enteric eukaryotic DNA viruses in specific pathogen free C57BL/6N mice. Res Vet Sci 2021; 136:1–5.

43. Raghupathi W, Raghupathi V. An Empirical Study of Chronic Diseases in the United States: A Visual Analytics Approach to Public Health. Int J Environ Res Public Health [Internet] 2018 [cited 2023 Mar 10]; 15. Available from: /pmc/articles/PMC5876976/

44. Reynolds R, Dennis S, Hasan I, Slewa J, Chen W, Tian D, Bobba S, Zwar N. A systematic review of chronic disease management interventions in primary care. BMC Fam Pract [Internet] 2018 [cited 2023 Mar 10]; 19. Available from: /pmc/articles/PMC5759778/

45. Powell EE, Wong VWS, Rinella M. Non-alcoholic fatty liver disease. The Lancet 2021; 397:2212–24.

46. Nomiyama T, Perez-Tilve D, Ogawa D, Gizard F, Zhao Y, Heywood EB, Jones KL, Kawamori R, Cassis LA, Tschöp MH, et al. Osteopontin mediates obesity-induced adipose tissue macrophage infiltration and insulin resistance in mice. J Clin Invest 2007; 117:2877.

47. Lesniewski LA, Hosch SE, Neels JG, De Luca C, Pashmforoush M, Lumeng CN, Chiang SH, Scadeng M, Saltiel AR, Olefsky JM. Bone marrow–specific Cap gene deletion protects against high-fat diet–induced insulin resistance. Nature Medicine 2007 13:4 2007; 13:455–62.

48. Weisberg SP, McCann D, Desai M, Rosenbaum M, Leibel RL, Ferrante AW. Obesity is associated with macrophage accumulation in adipose tissue. J Clin Invest [Internet] 2003 [cited 2023 Mar 10]; 112:1796–808. Available from: http://www.insightful.

49. Sutti S, Locatelli I, Bruzzì S, Jindal A, Vacchiano M, Bozzola C, Albano E. CX3CR1-expressing inflammatory dendritic cells contribute to the progression of steatohepatitis. Clin Sci 2015; 129:797–808.

50. Fujisaka S. The role of adipose tissue M1/M2 macrophages in type 2 diabetes mellitus. Diabetol Int [Internet] 2020 [cited 2023 Mar 10]; 12:74–9. Available from: https://pubmed.ncbi.nlm.nih.gov/33479582/

51. Guarner V, Rubio-Ruiz ME. Low-Grade Systemic Inflammation Connects Aging, Metabolic Syndrome and Cardiovascular Disease. Interdiscip Top Gerontol 2015; 40:99–106.

52. Mansyur MA, Bakri S, Patellongi IJ, Rahman IA. The association between metabolic syndrome components, low-grade systemic inflammation and insulin resistance in non-diabetic Indonesian adolescent male. Clin Nutr ESPEN 2020; 35:69–74.

53. Tangvarasittichai S, Pongthaisong S, Tangvarasittichai O. Tumor Necrosis Factor-A, Interleukin-6, C-Reactive Protein Levels and Insulin Resistance Associated with Type 2 Diabetes in Abdominal Obesity Women. Indian J Clin Biochem 2016; 31:68–74.

54. Kakino S, Ohki T, Nakayama H, Yuan X, Otabe S, Hashinaga T, Wada N, Kurita Y, Tanaka K, Hara K, et al. Pivotal Role of TNF-α in the Development and Progression of Nonalcoholic Fatty Liver Disease in a Murine Model. Hormone and Metabolic Research 2018; 50:80–7.

55. Stanley TL, Zanni M V., Johnsen S, Rasheed S, Makimura H, Lee H, Khor VK, Ahima RS, Grinspoon SK. TNF-α Antagonism with Etanercept Decreases Glucose and Increases the Proportion of High Molecular Weight Adiponectin in Obese Subjects with Features of the Metabolic Syndrome. J Clin Endocrinol Metab 2011; 96:E146–50.

56. Qin CC, Liu YN, Hu Y, Yang Y, Chen Z. Macrophage inflammatory protein-2 as mediator of inflammation in acute liver injury. World J Gastroenterol 2017; 23:3043–52.

57. Sun L, Ma L, Ma Y, Zhang F, Zhao C, Nie Y. Insights into the role of gut microbiota in obesity: pathogenesis, mechanisms, and therapeutic perspectives. Protein Cell 2018; 9:397–403.

58. Armougom F, Henry M, Vialettes B, Raccah D, Raoult D. Monitoring Bacterial Community of Human Gut Microbiota Reveals an Increase in Lactobacillus in Obese Patients and Methanogens in Anorexic Patients. PLoS One 2009; 4:e7125.

59. Xu P, Li M, Zhang J, Zhang T. Correlation of intestinal microbiota with overweight and obesity in Kazakh school children. BMC Microbiol 2012; 12:283.

60. Bervoets L, Van Hoorenbeeck K, Kortleven I, Van Noten C, Hens N, Vael C, Goossens H, Desager KN, Vankerckhoven V. Differences in gut microbiota composition between obese and lean children: a cross-sectional study. Gut Pathog 2013; 5:10.

61. Duarte SMB, Stefano JT, Miele L, Ponziani FR, Souza-Basqueira M, Okada LSRR, de Barros Costa FG, Toda K, Mazo DFC, Sabino EC, et al. Gut microbiome composition in lean patients with NASH is associated with liver damage independent of caloric intake: A prospective pilot study. Nutrition, Metabolism and Cardiovascular Diseases 2018; 28:369–84.

62. Raman M, Ahmed I, Gillevet PM, Probert CS, Ratcliffe NM, Smith S, Greenwood R, Sikaroodi M, Lam V, Crotty P, et al. Fecal microbiome and volatile organic compound metabolome in obese humans with nonalcoholic fatty liver disease. Clinical Gastroenterology and Hepatology 2013; 11:868-875.e3.

63. Da Silva HE, Teterina A, Comelli EM, Taibi A, Arendt BM, Fischer SE, Lou W, Allard JP. Nonalcoholic fatty liver disease is associated with dysbiosis independent of body mass index and insulin resistance. Scientific Reports 2018 8:1 2018; 8:1–12.

64. Guo WL, Chen M, Pan WL, Zhang Q, Xu JX, Lin YC, Li L, Liu B, Bai WD, Zhang YY, et al. Hypoglycemic and hypolipidemic mechanism of organic chromium derived from chelation of Grifola frondosa polysaccharide-chromium (III) and its modulation of intestinal microflora in high fat-diet and STZ-induced diabetic mice. Int J Biol Macromol 2020; 145:1208–18.

65. van Muijlwijk GH, van Mierlo G, Jansen PWTC, Vermeulen M, Bleumink-Pluym NMC, Palm NW, van Putten JPM, de Zoete MR. Identification of Allobaculum mucolyticum as a novel human intestinal mucin degrader. Gut Microbes 2021; 13.

66. Cox LM, Yamanishi S, Sohn J, Alekseyenko A V., Leung JM, Cho I, Kim SG, Li H, Gao Z, Mahana D, et al. Altering the Intestinal Microbiota during a Critical Developmental Window Has Lasting Metabolic Consequences. Cell 2014; 158:705–21.

67. Zhang X, Zhao Y, Zhang M, Pang X, Xu J, Kang C, Li M, Zhang C, Zhang Z, Zhang Y, et al. Structural Changes of Gut Microbiota during Berberine-Mediated Prevention of Obesity and Insulin Resistance in High-Fat Diet-Fed Rats. PLoS One [Internet] 2012 [cited 2023 Mar 10];

7:e42529. Available from: https://journals.plos.org/plosone/article?id=10.1371/journal.pone.0042529

68. Scheithauer TPM, Rampanelli E, Nieuwdorp M, Vallance BA, Verchere CB, van Raalte DH, Herrema H. Gut Microbiota as a Trigger for Metabolic Inflammation in Obesity and Type 2 Diabetes. Front Immunol [Internet] 2020 [cited 2023 Mar 10]; 11:571731. Available from: /pmc/articles/PMC7596417/

69. Prince AM, Horowitz B, Brotman B. Sterilisation of hepatitis and HTLV-III viruses by exposure to tri(n-butyl)phosphate and sodium cholate. Lancet 1986; 1:706–10.

70. Remy MM, Alfter M, Chiem M-N, Barbani MT, Engler OB, Suter-Riniker F. Effective chemical virus inactivation of patient serum compatible with accurate serodiagnosis of infections. Clin Microbiol Infect 2019; 25:907.e7-907.e12.

71. WHO Health Product Policy and Standards Team. Guidelines on viral inactivation and removal procedures intended to assure the viral safety of human blood plasma products [Internet]. 2004 [cited 2023 Jan 2]; :WHO-TRS924-Annex4-1-82. Available from: https://www.who.int/publications/m/item/WHO-TRS924-Annex4

72. Trescec A, Simić M, Branović K, Gebauer B, Benko B. Removal of detergent and solvent from solvent-detergent-treated immunoglobulins. J Chromatogr A 1999; 852:87–91.

73. Pettersson US, Waldén TB, Carlsson PO, Jansson L, Phillipson M. Female Mice are Protected against High-Fat Diet Induced Metabolic Syndrome and Increase the Regulatory T Cell Population in Adipose Tissue. PLoS One 2012; 7.

74. Edgar RC. Updating the 97% identity threshold for 16S ribosomal RNA OTUs. Bioinformatics 2018; 34:2371–5.

75. Edgar R. SINTAX: a simple non-Bayesian taxonomy classifier for 16S and ITS sequences. bioRxiv [Internet] 2016 [cited 2018 Jun 5]; :074161. Available from: https://doi.org/10.1101/074161

76. Kim O-S, Cho Y-J, Lee K, Yoon S-H, Kim M, Na H, Park S-C, Jeon YS, Lee J-H, Yi H, et al. Introducing EzTaxon-e: a prokaryotic 16S rRNA gene sequence database with phylotypes that represent uncultured species. Int J Syst Evol Microbiol 2012; 62:716–21.

77. Bolger AM, Lohse M, Usadel B. Trimmomatic: A flexible trimmer for Illumina sequence data. Bioinformatics 2014; 30:2114–20.

78. Bankevich A, Nurk S, Antipov D, Gurevich AA, Dvorkin M, Kulikov AS, Lesin VM, Nikolenko SI, Pham S, Prjibelski AD, et al. SPAdes: a new genome assembly algorithm and its applications to single-cell sequencing. Journal of Computational Biology 2012; 19:455–77.

79. Guo J, Bolduc B, Zayed AA, Varsani A, Dominguez-Huerta G, Delmont TO, Pratama AA, Gazitúa MC, Vik D, Sullivan MB, et al. VirSorter2: a multi-classifier, expert-guided approach to detect diverse DNA and RNA viruses. Microbiome 2021; 9:37.

80. Kieft K, Zhou Z, Anantharaman K. VIBRANT: automated recovery, annotation and curation of microbial viruses, and evaluation of viral community function from genomic sequences. Microbiome 2020; 8:90.

81. Nayfach S, Camargo AP, Schulz F, Eloe-Fadrosh E, Roux S, Kyrpides NC. CheckV assesses the quality and completeness of metagenome-assembled viral genomes. Nat Biotechnol 2021; 39:578–85.

82. Pasolli E, Asnicar F, Manara S, Zolfo M, Karcher N, Armanini F, Beghini F, Manghi P, Tett A, Ghensi P, et al. Extensive unexplored human microbiome diversity revealed by over 150,000 genomes from metagenomes spanning age, geography, and lifestyle. Cell 2019; 176:649-662.e20.

83. Castro-Mejía JL, Khakimov B, Lind M V, Garne E, Paulová P, Tavakkoli E, Hansen LH, Smilde AK, Holm L, Engelsen SB, et al. Gut microbiome and its cofactors are linked to lipoprotein distribution profiles. bioRxiv 2021; :2021.09.01.458531.

84. Langmead B, Salzberg SL. Fast gapped-read alignment with Bowtie 2. Nat Methods 2012; 9:357–9.

85. Paulson JN, Stine OC, Bravo HC, Pop M. Differential abundance analysis for microbial marker-gene surveys. Nat Methods 2013; 10:1200–2.

86. Weiss S, Xu ZZ, Peddada S, Amir A, Bittinger K, Gonzalez A, Lozupone C, Zaneveld JR, Vázquez-Baeza Y, Birmingham A, et al. Normalization and microbial differential abundance strategies depend upon data characteristics. Microbiome 2017; 5:27.

87. Paulson J. metagenomeSeq: Statistical analysis for sparse high-throughput sequencing. BioconductorJp 2014; :1–20.

88. Team RC. R: A language and environment for statistical title.

89. McMurdie PJ, Holmes S. phyloseq: an R package for reproducible interactive analysis and graphics of microbiome census data. PLoS One 2013; 8:e61217.

90. Dixon P. VEGAN, a package of R functions for community ecology. Journal of Vegetation Science 2003; 14:927–30.

91. Love MI, Huber W, Anders S. Moderated estimation of fold change and dispersion for RNA-seq data with DESeq2. Genome Biol 2014; 15:550.

92. Andersen KS, Kirkegaard RH, Karst SM, Albertsen M. ampvis2: an R package to analyse and visualise 16S rRNA amplicon data. bioRxiv 2018;

93. Wickham H. ggplot2. Wiley Interdiscip Rev Comput Stat 2011; 3:180–5.

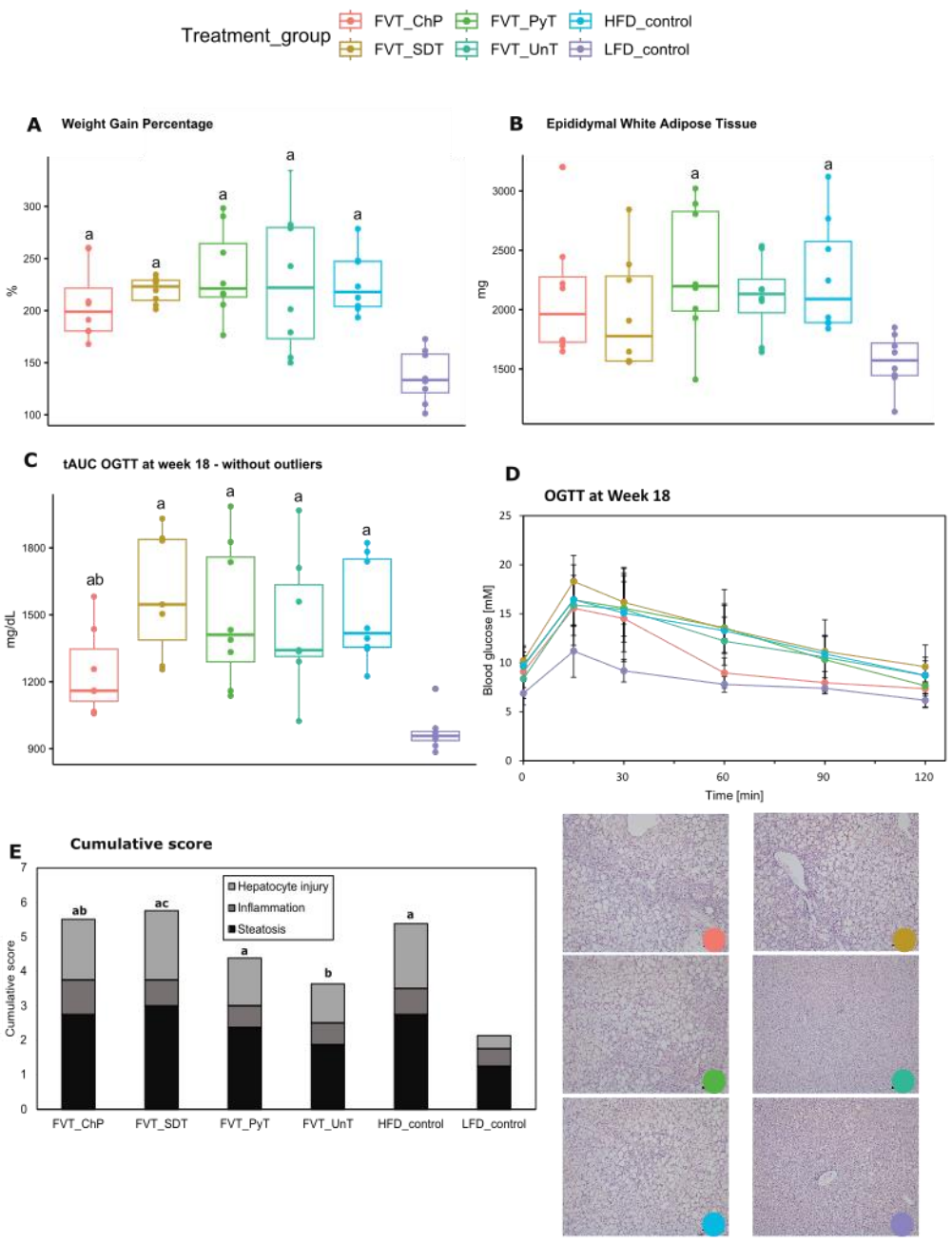

Figure 1: Overview of mouse phenotypic characteristics. A) Weight gain percentage of the mice treated with the four different FVT treatments. B) Measure of epididymal white adipose tissue isolated from mice from the different FVT treatment groups. C) and D) Oral glucose tolerance test (OGTT) and total area under the curve (tAUC) measured 10 weeks after second FVT (23 weeks old) of the different FVT treatment groups. E) Cumulative score and representative histology images of liver tissue evaluating the effect of the different FVT treatments related to liver pathology. Significant changes compared to LFD-control treatment, HFD-control, and FVT-UnT are marked by (a), (b), and (c), respectively. Scale in histology images = 300 µm.

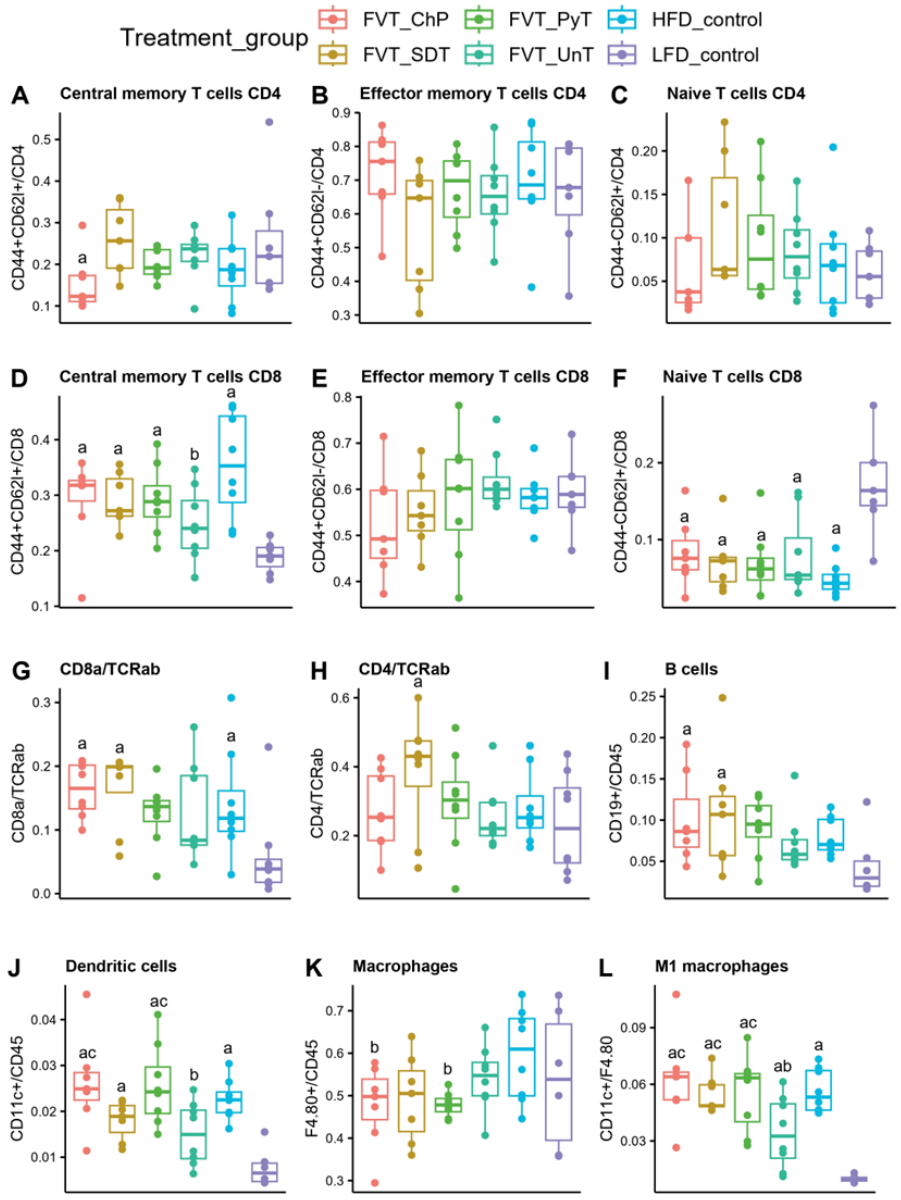

744

745 Figure 2: Immune cell count in fat tissue at study termination. A) to L) are showing the overall fluorescence-activated cell
746 sorter (FACS) profile in the mouse fat tissue of the different FVT treatments. Significant changes compared to LFD-control
747 treatment, HFD-control and FVT-UnT are marked by (a), (b), and (c), respectively.

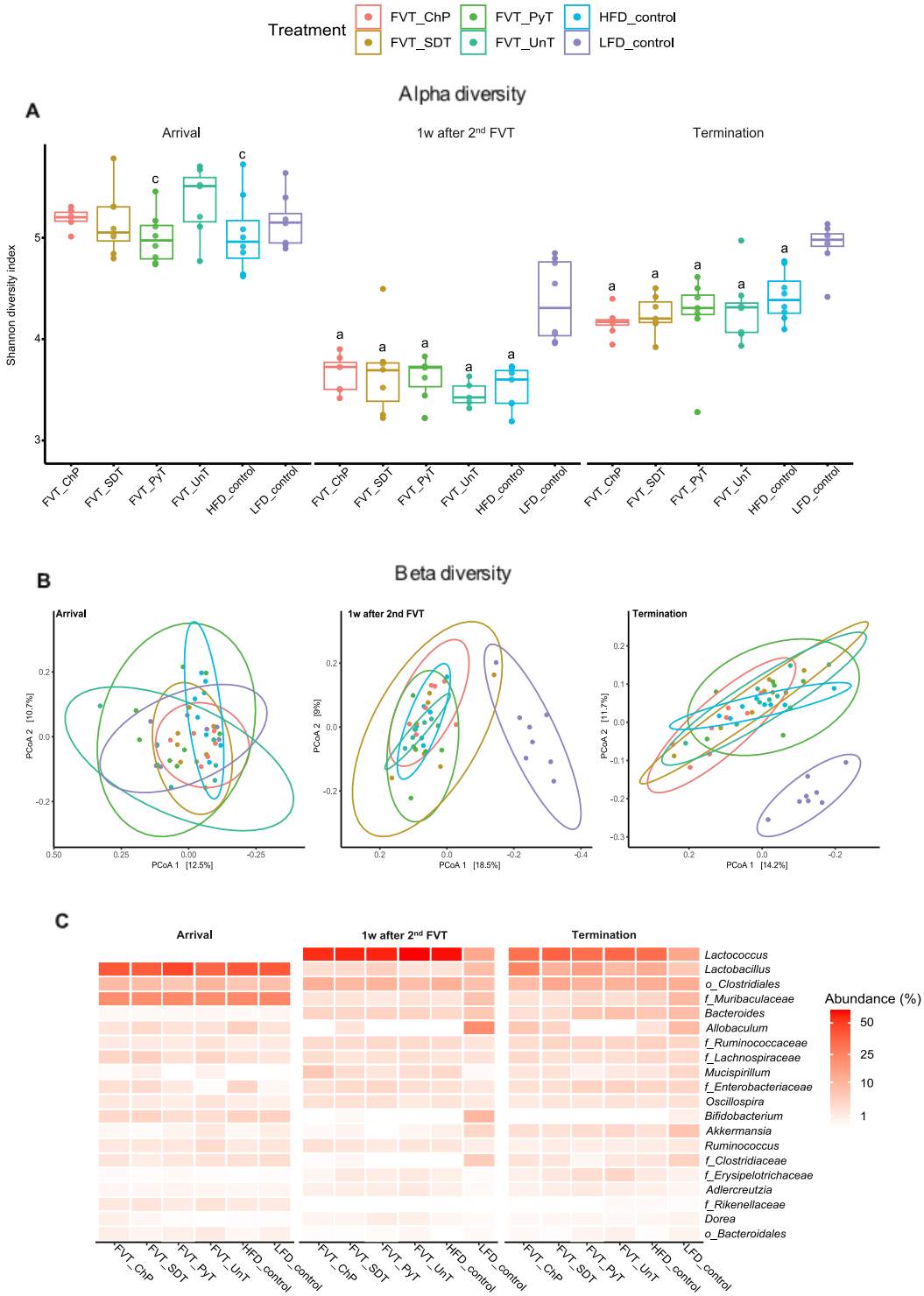

Figure 3: Bacteriome analysis based on 16S rRNA gene amplicon sequencing. A) The general bacterial Shannon diversity index (alpha diversity), B) bray-curtis dissimilarity based PCoA plot (beta diversity) and C) heatmap representing the relative abundance of dominating bacterial taxa at arrival (before diet intervention, age week 5), one week after the second FVT (1w after 2nd FVT, age week 14), and termination (age week 23). Significant changes compared to LFD-control treatment, HFD-control and FVT-UnT are marked by (a), (b), and (c), respectively.

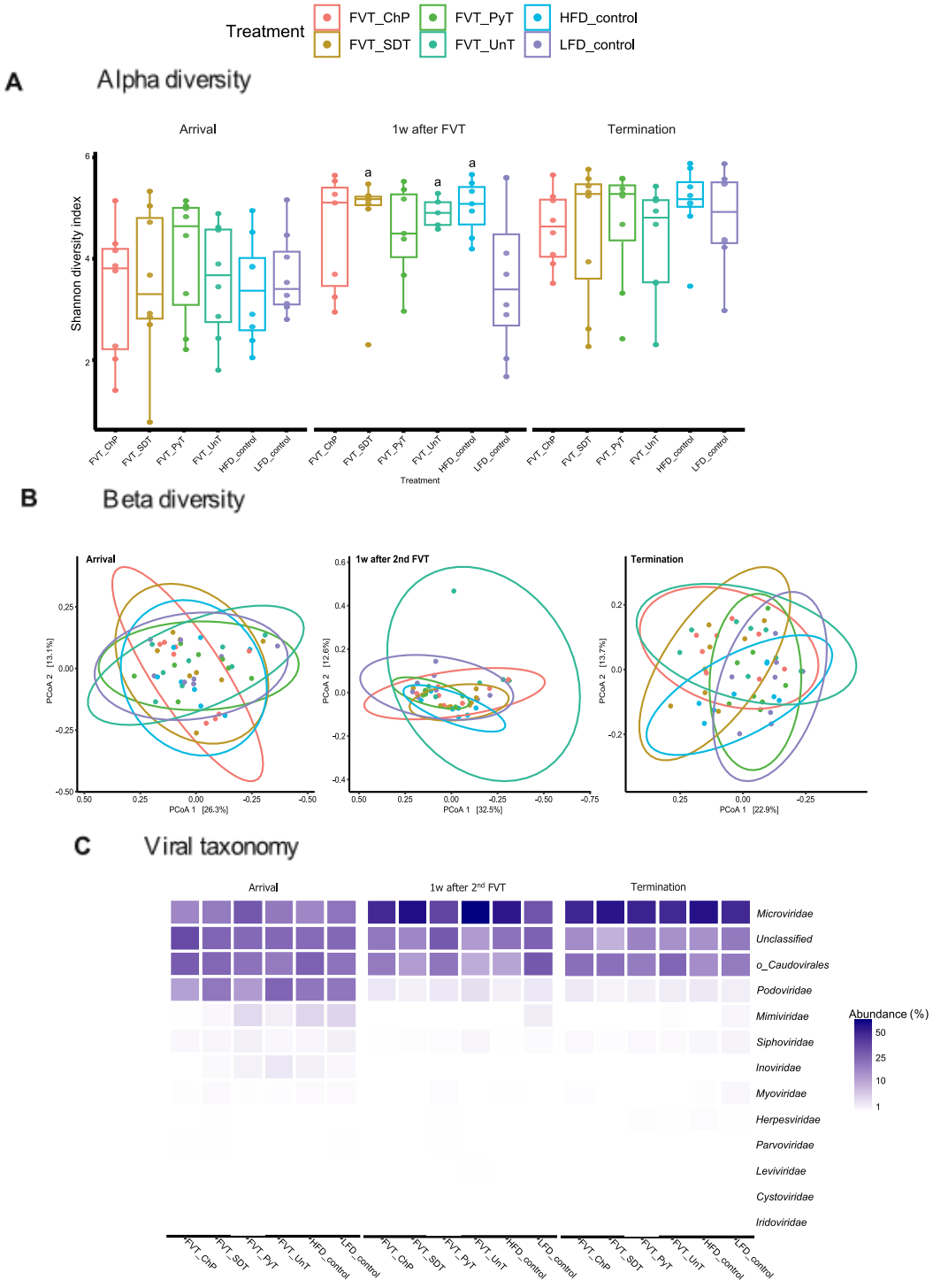

Figure 4: Metavirome analysis based on whole-genome sequencing of viral entities. A) The general viral Shannon diversity indexes (alpha diversity), B) Bray-curtis dissimilarity based PCoA plot (beta diversity), C) heatmap representing the relative abundance of dominating viral taxa at arrival (before diet intervention, age week 5), one week after the second FVT (1w after 2nd FVT, age week 14), and termination (age week 23). Significant changes compared to LFD-control treatment, HFD-control and FVT-UnT are marked by (a), (b), and (c), respectively.

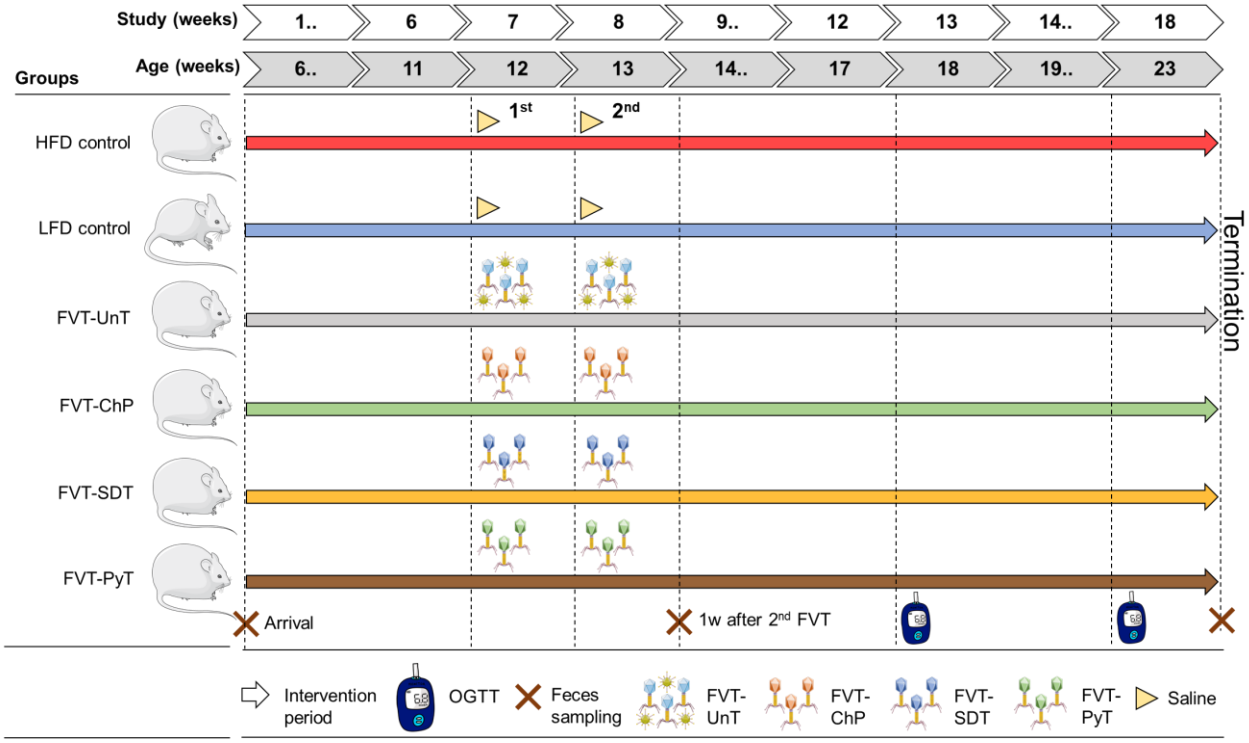

Figure 5: Overview of the animal model. Forty-eight male C57BL/6NTac mice (5 weeks old) were divided into six groups. The mice were fed with either low-fat diet and high-fat diet. After six and seven weeks on a high-fat diet, the mice were treated with either FVT-UnT (fecal virome transplantation with untreated sterile filtered donor feces from heathy mice), FVT_ChP (FVT with chemostat propagation of fecal donor virome to remove eukaryotic viruses by gradient dilution), FVT_SDT (FVT with solvent detergent treatment to inactive enveloped viruses), and FVT_PyT (FVT with pyronin Y treatment to inactive RNA viruses), or a saline solution as sham. Oral glucose tolerance tests (OGTT) were measured at week 18 and 23 of age. The brown crosses mark the timepoint of feces samples that were used for gut microbiome analysis.